

Photostabilized Chlorophyll *a* in Mesoporous Silica: Adsorption Properties and Photoreduction Activity of Chlorophyll *a*

Tetsuji Itoh,^{*,†} Kazuhisa Yano,[†] Yuji Inada,[‡] and Yoshiaki Fukushima[†]

Contribution from the Toyota Central R & D Labs Inc., Yokomichi, Nagakute, Aichi 480-1192, Japan, and Toin Human Science and Technology Center, Toin University of Yokohama, Kurogane-cho, Aoba-ku, Yokohama 225-8502, Japan

Received February 26, 2002. Revised Manuscript Received August 26, 2002

Abstract: Chlorophyll *a* was adsorbed to mesoporous silica (FSM, folded-sheet mesoporous material) to form a chlorophyll–FSM conjugate, in which a nanometer-scale interaction between chlorophyll *a* molecules resembles a living plant leaf. The mesopores of FSM acted as nanoscale spaces not only for an interaction between chlorophyll molecules and the silica support but also for a nanoscale interaction between the adsorbed chlorophyll molecules. These interactions contribute to photostability. An increase in the amount of chlorophyll adsorbed to the pores of FSM leads to an enhancement of the photostability accompanied by a shift in the absorbance maximum to a longer wavelength. The physiological function of the chlorophyll–FSM conjugate was explored as chlorophyll–FSM exhibited the photoinduced ability to catalyze the reduction of methyl viologen (an electron carrier). The evolution of hydrogen gas was observed for 14 h without deterioration when an aqueous suspension containing chlorophyll–FSM, methyl viologen, 2-mercaptoethanol (an electron donor), and platinum was illuminated with visible light.

Introduction

A large number of investigations on photosensitization have been performed with photocatalytic inorganic compounds such as titanium oxide (TiO₂),^{1–3} silicon carbide (SiC),⁴ and strontium titanate (SrTiO₃)⁵ illuminated with ultraviolet rays. Organic photocatalysts such as chlorophyll and porphyrin derivatives that act under visible light illumination are very useful as catalysts.^{6–10} However, natural chlorophylls extracted from living leaves have been seldom used as photocatalysts because of their instability. In the layered thylakoid membrane of chloroplasts in intact leaves, chlorophyll molecules bind to proteins to form chlorophyll–protein conjugates in which the chlorophyll–protein interactions and nanoscale chlorophyll–chlorophyll interactions play an important role in stabilization

and physiological functions of living plant leaves; i.e., the photolysis of water and the reduction of NADP¹¹ by sunlight illumination. Itoh and co-workers have reported that chlorophyll *a* adsorbed to silicate layers of smectite showed photostable and photocatalyzed properties,^{12–14} which demonstrated the importance of chlorophyll–support interactions.

Currently, there is great interest in mesoporous materials such as MCM (mobile crystalline material)¹⁵ and FSM (folded-sheet mesoporous material)¹⁶ having honeycomb (hexagonal) structures with ordered cylindrical channels of 2–10 nm diameter, which is larger than the microporous cavities of conventional zeolites (0.6–1.2 nm). They are potential hosts for the inclusion of bulky organometallic and inorganic complexes and offer nanoscale spaces to synthesize robust metal clusters such as Pt nanowires.¹⁷ Furthermore, mesoporous ordered channels (2–10 nm diameter) can uniformly occlude not only some larger metal complexes such as porphyrin^{18–21} and phthalocyanine²²

* To whom correspondence should be addressed: e-mail t_ito@mosk.tytlabs.co.jp.

[†] Toyota Central R & D Labs Inc.

[‡] Toin University of Yokohama.

- (1) Yoneyama, H.; Koizumi, M.; Tamura, H. *Bull. Chem. Soc. Jpn.* **1979**, *52*, 3449–3450.
- (2) Takata, T.; Shinohara, K.; Tanaka, A.; Hara, M.; Kondo, J. N.; Domen, K. *J. Photochem. Photobiol. A: Chem.* **1997**, *106*, 45–49.
- (3) Takata, T.; Furumi, Y.; Shinohara, K.; Tanaka, A.; Hara, M.; Kondo, J. N.; Domen, K. *Chem. Mater.* **1997**, *9*, 1063–1064.
- (4) Inoue, T.; Fujishima, A.; Konishi, S.; Honda, K. *Nature* **1979**, *277*, 637–638.
- (5) Aurian-Blajeni, B.; Halmann, M.; Manassen, J. *Solar Energy* **1980**, *25*, 165–170.
- (6) Willner, I.; Mandler, D. *Enzyme Microb. Technol.* **1989**, *11*, 467–483.
- (7) Mandler, D.; Willner, I. *J. Am. Chem. Soc.* **1984**, *106*, 5352–5353.
- (8) Mandler, D.; Willner, I. *J. Chem. Soc., Chem. Commun.* **1986**, 851–853.
- (9) Okura, I.; Kaji, N.; Aono, S.; Kita, T.; Yamada, A. *Inorg. Chem.* **1985**, *24*, 451–453.
- (10) Okura, I.; Kusunoki, S.; Aono, S. *Bull. Chem. Soc. Jpn.* **1984**, *57*, 1184–1188.

- (11) Scheer, H. *Chlorophylls*; Scheer, H., Ed.; CRC Press: London, 1991.
- (12) Kodera, Y.; Kageyama, H.; Sekine, H.; Inada, Y. *Biotechnol. Lett.* **1992**, *14*, 119–122.
- (13) Ishii, A.; Itoh, T.; Kageyama, H.; Mizoguchi, T.; Kodera, Y.; Matsushima, A.; Torii, K.; Inada, Y. *Dyes Pigments* **1995**, *28*, 77–82.
- (14) Itoh, T.; Ishii, A.; Kodera, Y.; Matsushima, A.; Hiroto, M.; Nishimura, H.; Tsuzuki, T.; Kamachi, T.; Okura, I.; Inada, Y. *Bioconjugate Chem.* **1998**, *9*, 409–412.
- (15) Kresge, C. T.; Leonowicz, M. E.; Roth, W. J.; Vartuli, J. C.; Beck, J. S. *Nature* **1992**, *359*, 710.
- (16) Inagaki, S.; Fukushima, Y.; Kuroda, K. *J. Chem. Soc., Chem. Commun.* **1993**, 680–682.
- (17) Sasaki, M.; Osada, M.; Sugimoto, N.; Inagaki, S.; Fukushima, Y.; Fukuoka, A.; Itikawa, M. *Microporous Mesoporous Mater.* **1998**, *21*, 597–606.
- (18) Murata, S.; Furukawa, H.; Kuroda, K. *Chem. Mater.* **2001**, *13*, 2722–2729.
- (19) Tachibana, J.; Chiba, M.; Itikawa, M.; Inamura, T.; Sasaki, Y. *Supramol. Sci.* **1998**, *5*, 281–287.

but also enzymes such as peroxidase²³ and trypsin²⁴ to form supramolecular hybrid composites. Nanostructured composite materials have been studied for their abilities and stabilities. Interaction between support and adsorbed molecules or two molecules in these nano spaces should be an interesting subject for examination in order to understand the amazing properties of natural chlorophylls or enzymes.

The present paper deals with the preparation of a chlorophyll–FSM conjugate with high photostability. The mesopore spaces of the FSM also allow nanoscale interactions between the adsorbed chlorophyll molecules. Furthermore, the conjugate is found to evolve hydrogen gas effectively in the presence of an electron donor, a carrier, and a catalyst on visible light illumination.

Experimental Section

General. Chlorophyll *a* purified from *Spirulina*, L-lysine, poly(vinylpyrrolidone) with an average molecular weight of 10 000 (PVP), and methyl viologen (1,1-dimethyl-4,4-bipyridinium chloride) were purchased from Wako Pure Chemical Industries, Ltd. (Osaka, Japan). Smectite powder (hectorite) was obtained from Co-op Chemical Co., Ltd. (Tokyo, Japan). Silica gel (surface area 650 m²/g) was supplied by Fujisirisia Kagaku Co. Ltd. (Aichi, Japan). The mesoporous FSM-16 material, with a pore diameter of 2.7 nm, was prepared from kanemite (layered polysilicate) by use of hexadecyltrimethylammonium chloride, according to the method reported by Inagaki et al.¹⁶ The FSM was suspended in a 0.1% NaOH methanol solution for 3 min to prepare Na-FSM. The resulting product was filtered out, washed with methanol, and then air-dried at 50 °C.

Characterization. The absorption spectrum was measured on a Shimadzu (Kyoto, Japan) spectrophotometer MPS-2400. X-ray diffraction (XRD) patterns were obtained on a Rigaku RINT-2200 diffractometer with Cu K α radiation. The ²⁹Si NMR spectra were recorded on a Bruker MSL-300WB spectrometer at 59.62 MHz. Chemical shifts for ²⁹Si were referenced to trimethylsilane (TMS) at 0 ppm. Nitrogen adsorption isotherms were measured at 77 K with a Quantachrome Autosorb-1. Specific surface areas were calculated by the BET method with adsorption data ranging from $P/P_0 = 0.05$ to 0.35, and the pore size distribution curves were analyzed with the adsorption branch by the BJH method.

Preparation of the Chlorophyll–FSM Conjugate. A chlorophyll–FSM conjugate, Chl–FSM, was prepared as follows. Na-FSM (100 mg) was added to 2.0 mL of chlorophyll *a* dissolved in benzene (0–32.5 mM). Then the suspension was shaken for 30 min at 25 °C to establish an adsorption equilibrium. The chlorophyll–FSM conjugate was collected by centrifugation and then dried under reduced pressure. The amount of chlorophyll *a* adsorbed to the pores of the FSM was spectrophotometrically determined by measuring the absorbance of supernatant solutions after centrifugation at 665 nm, which is characteristic of the absorption band of chlorophyll *a*. The molar extinction coefficient (ϵ) of chlorophyll *a* was $9.25 \times 10^4 \text{ M}^{-1} \text{ cm}^{-1}$ at 661.6 nm in acetone.²⁵ The chlorophyll–FSM conjugate was collected by centrifugation and then dried under reduced pressure, followed by suspension in water. The chlorophyll was not extracted from chlorophyll–FSM in water. The molar extinction coefficient of chlorophyll–FSM in 0.1 M Tris-HCl buffer (pH 7.4) was determined to be $\epsilon_{675\text{nm}} =$

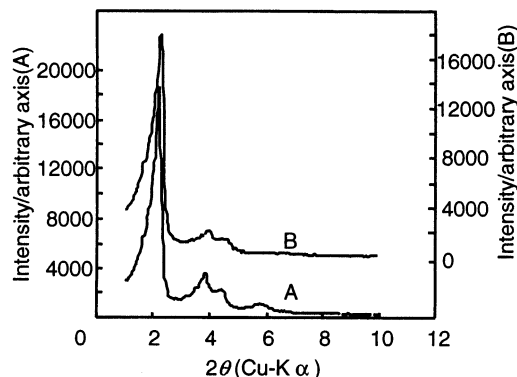


Figure 1. XRD patterns of FSM (A) and Na-FSM (B).

$5.0 \times 10^4 \text{ M}^{-1} \text{ cm}^{-1}$. Chlorophyll was seldom agglomerated outside FSM, which was proven by analysis with a picosecond streak camera system.

Photostability of Chlorophyll–FSM. The photostability of chlorophyll *a* was examined by illuminating the chlorophyll–FSM conjugate in water, as well as free chlorophyll *a* in benzene, with a 60 W incandescent lamp at a distance of 10 cm. The light intensity on a sample was approximately $200 \text{ J m}^{-2} \text{ s}^{-1}$. During the illumination, the sample was shielded from heat by the circulation of cold water.

Photoreduction of Methyl Viologen. The photoreduction of methyl viologen was examined in the presence of l-lysine, poly(vinylpyrrolidone), and 2-mercaptoethanol. The conjugate (0.38 mg; 0.1 μmol as chlorophyll) was suspended in 3 mL of 50 mM Tris-HCl buffer (pH 7.4) containing 0.1 M methyl viologen, 0.2 M l-lysine, 1.6 mM poly(vinylpyrrolidone), and 1 mmol of 2-mercaptoethanol. The sample mixture was deaerated by repeated freeze–pump–thaw cycles and then illuminated with a 60 W incandescent lamp at a distance of 3.5 cm. The light intensity was $1500 \text{ J m}^{-2} \text{ s}^{-1}$ at 30 °C. Light wavelengths less than 490 nm were cut out by use of a Toshiba L-49 filter (Tokyo, Japan). The photochemical reduction of methyl viologen was observed by measuring the increase in absorbance at 605 nm, with a molar extinction coefficient of $1.65 \times 10^{-1} \text{ M}^{-1} \text{ cm}^{-1}$.

Evolution of Hydrogen Gas. Hydrogen evolution by Chl–FSM in the presence of methyl viologen, l-lysine, poly(vinylpyrrolidone), sodium carbonate, 2-mercaptoethanol, and platinum was examined according to the method described by Okura et al.^{9,10} The reaction system (80 mL) consisted of 200 mg of Chl–FSM suspended in 50 mM Tris-HCl buffer (pH 7.4) in the presence of methyl viologen (50 mM), l-lysine (0.1 M), poly(vinylpyrrolidone) (1.6 mM), sodium carbonate (0.1 M), 2-mercaptoethanol (1 mmol), and platinum (0.6 mg). The sample mixture was placed in a Pyrex glass cell (694.6 cm³), equipped with a magnetic stirrer, and was deaerated. Then the upper space of the cell (614.6 cm³) was filled with argon gas (600 Torr). The sample in the cell was illuminated with a 500 W xenon lamp (light intensity $380 \text{ J m}^{-2} \text{ s}^{-1}$). Light wavelengths less than 400 nm were cut out with a Toshiba L-39 filter (Tokyo, Japan). A portion of the evolved hydrogen gas was collected via a sampling valve on the cell and then analyzed by gas chromatography.

Results and Discussion

XRD and NMR. The XRD patterns of FSM (A) and Na-FSM (B) are shown in Figure 1. Low-angle diffraction peaks for (100), (110), (200), and (210) were observed, which confirmed the highly ordered hexagonal mesopore arrangement. The hexagonal structure of Na-FSM was maintained by 0.1% NaOH methanol treatment. Figure 2 shows the ²⁹Si magic-angle spinning (MAS) NMR spectra of FSM (A) and Na-FSM (B). The two resonances at –109 and –102 ppm, which were

- (20) Zhou, H. S.; Honma, I. *Chem. Lett.* **1998**, 973–974.
 (21) Xu, W.; Guo, H.; Akins, D. L. *J. Phys. Chem. B.* **2001**, *105*, 1543–1546.
 (22) Armengol, E.; Corma, A.; Fornes, V.; Garcia, H.; Primo, J. *Appl. Catal. A* **1999**, *108*, 305–312.
 (23) Takahashi, H.; Li, B.; Sasaki, T.; Miyazaki, C.; Kajino, T.; Inagaki, S. *Chem. Mater.* **2000**, *12*, 3301–3305.
 (24) Yiu, H. H. P.; Wright, P. A.; Botting, N. P. *J. Mol. Catal. B: Enzym.* **2001**, *15*, 81–92.
 (25) Lichtenthaler, H. K. *Methods Enzymol.* **1987**, *148*, 350–382.

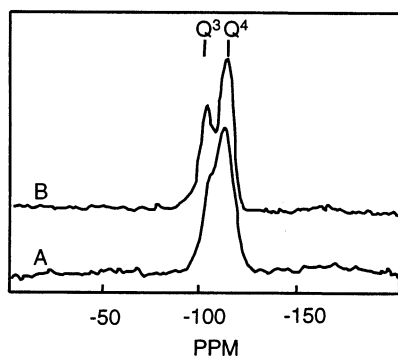


Figure 2. ^{29}Si MAS NMR spectra of FSM (A) and Na-FSM (B).

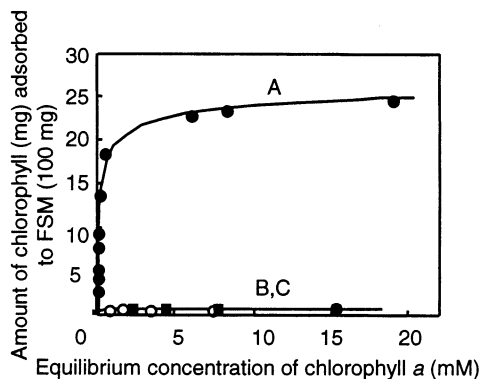


Figure 3. Adsorption of chlorophyll *a* to the pores of FSM powder (A), silica gel (B), and smectite (C) in benzene was spectrophotometrically measured with respect to the equilibrium concentration of chlorophyll *a*.

assigned to the silicon sites of Q^4 , $\text{Si}(\text{OSi})_4$, and Q^3 , $\text{HOSi}(\text{OSi})_3$, respectively, were observed for the FSM (curve A). The bands for Na-FSM are sharper than those for FSM, which suggested an exchange of H^+ of FSM for Na^+ .

Adsorption Isotherm. The adsorption of chlorophyll *a* in the pores of FSM powder, silica gel, and smectite in benzene were spectrophotometrically measured with respect to the equilibrium concentration of chlorophyll *a* (Figure 3). The adsorption proceeded efficiently with the equilibrium concentration of chlorophyll *a* and reached a constant level with an adsorption equilibrium at 6 mM (curve A). In this case, 23 mg of the 57 mg of chlorophyll *a* was adsorbed in the pores of FSM (100 mg) in benzene. On the other hand, the amounts of chlorophyll *a* adsorbed to the silica gel and smectite were low in comparison with that on FSM (curves B and C). These results can be attributed to the high surface area and suitable pore size of FSM.

Nitrogen Adsorption. By use of chlorophyll-FSM conjugates in which various amounts of chlorophyll *a* (0–24.6 mg) were adsorbed to the pores of FSM (100 mg), the nitrogen adsorption isotherms of chlorophyll-FSM were examined (Figure 4). With increasing amounts of chlorophyll *a* (0, 2.6, 9.5, 18.4, and 24.6 mg) adsorbed to the pores of FSM (100 mg), the amount of nitrogen adsorbed to chlorophyll-FSM decreased, which is shown by curves A–E, respectively. A steep increase in nitrogen uptake at the relative pressure of 0.3 can be seen for FSM, which was due to capillary condensation (curve A). On the other hand, the nitrogen uptake by chlorophyll-FSM is low in comparison with that by FSM (curve E). In this case, the pore volume of chlorophyll-FSM was ca. 6% that of the FSM. This indicates that the pores of FSM were filled with chlorophyll *a*.

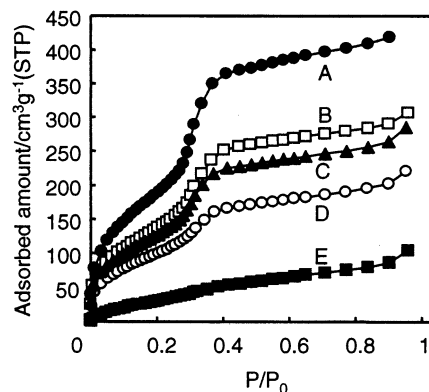


Figure 4. Changes in nitrogen adsorption isotherms with chlorophyll-FSM conjugates in which various amounts of chlorophyll *a* (0–24.6 mg) were adsorbed to the pores of FSM (100 mg) with an average pore size of 2.7 nm. Curves A–E: 0, 2.6, 9.5, 18.4, and 24.6 mg, respectively, of chlorophyll *a* was adsorbed to the pores of FSM (100 mg).

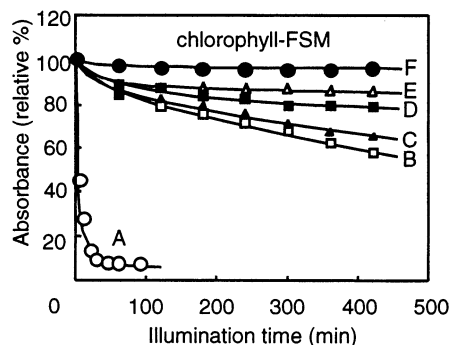


Figure 5. Photostability of chlorophyll *a* (Chl) and Chl-FSM. Curve A: Chlorophyll *a* in benzene. Curves B–F: Chl-FSM conjugates dispersed in water with absorption maxima of 671, 672, 673, 674, and 675 nm, respectively. Each sample was illuminated, at a light intensity of $200 \text{ J m}^{-2} \text{ s}^{-1}$, at 30°C .

Photostability of Chlorophyll-FSM. By use of chlorophyll-FSM conjugates in which various amounts of chlorophyll *a* (0–25 mg) were adsorbed to the pores of FSM (100 mg), photostability was examined by illumination with visible light. The results are shown in Figure 5. Free chlorophyll *a* in benzene, with an absorption maximum at 665 nm (curve A), was markedly discolored by the illumination. On the other hand, the chlorophyll-FSM conjugates in water were much more photostable in comparison with free chlorophyll. The photostabilization of the chlorophyll conjugates with absorption maxima at 671, 672, 673, 674, and 675 nm is shown by curves B–F, respectively. They became more photostable with increasing amounts of adsorbed chlorophyll *a*. A relative absorbance value of 96% is retained at the absorption maximum in the red region after 420 min of illumination, shown by curve F. On the other hand, chlorophyll-smectite, in which only 1 mg of chlorophyll was adsorbed to 100 mg of smectite, showed photostability resembling curve B. Therefore, the enhancement of the photostability of chlorophyll in conjugates seems to be accompanied not only by an interaction between chlorophyll and the support but also by an interaction between two chlorophyll molecules. The absorption spectra of chlorophyll *a* in benzene and two types of Chl-FSM in aqueous solution are shown in Figure 6 (curves A, B, and F, respectively). For curves B and F, 2 mg and 24 mg of chlorophyll *a* was adsorbed to the pores of FSM (100 mg). The wavelength of the absorption maximum is 665 nm for chlorophyll *a* in benzene and 671 and

Table 1. Physicochemical and Spectrophotometric Properties of the Chlorophyll–FSM Conjugate

	characteristics of host material			properties of chlorophyll–FSM				
	BJH pore diameter (nm)	pore volume (cm ³ g ⁻¹)	specific surface area (m ² g ⁻¹)	chlorophyll <i>a</i> adsorbed (mg/100 mg of FSM)	pore volume (cm ³ g ⁻¹)	specific surface area (m ² g ⁻¹)	absorption maximum (nm)	stabilization of chlorophyll <i>a</i> ^a (%)
FSM-16	2.7	0.53	742	24.6	0.05	140	675	97
				18.4	0.22	386	674	85
				9.5	0.31	489	673	78
				5.2			672	63
				2.6	0.41	529	671	58
silica gel ^b			650	0.7			671	
smectite ^b			160	1.0			673	62
chlorophyll <i>a</i> in benzene							665	<8
chlorophylls in intact leaves							678	100

^a Relative absorbance value at the absorption maximum in the red region after 360 min of illumination. The absorbance value of each sample obtained before the irradiation was regarded as 100%. ^b Adsorption of chlorophyll onto silica gel and smectite reaches a constant level with an adsorption equilibrium.

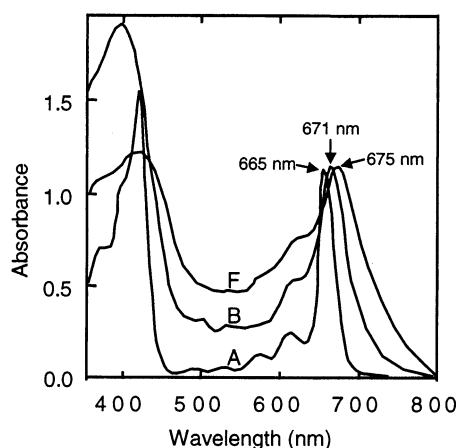


Figure 6. Absorption spectra of chlorophyll *a* (Chl). Curve A: Spectrum of chlorophyll *a* in benzene (absorption maximum of 665 nm). Curves B and F: Spectra of Chl–FSM in aqueous solution (absorption maxima of 671 and 675 nm, respectively).

675 nm for Chl–FSM in aqueous solution. Although absorption at 673 nm was also observed for the chlorophyll–smectite conjugate, none at the longer wavelength of 675 nm was observed. Table 1 shows the properties of the conjugates with different amounts of chlorophyll *a* adsorbed to the pores of FSM, the pore volumes, the specific surface areas, the absorption maxima, and the degrees of photostability. As is clear from the table, chlorophylls in intact leaves exhibit an absorption maximum at 678 nm²⁶ and are quite stable against illumination. On the contrary, chlorophyll *a* in benzene exhibits an absorption maximum of 665 nm and has no stability against illumination. It is noteworthy that the enhancement of photostability for the chlorophyll–FSM was accompanied by an increase in the amount of chlorophyll *a* adsorbed to the pores of FSM, together with decreases in the pore volume and specific surface area, and also by a shift in the absorption band to a longer wavelength. Such a shift in the absorption band is attributable to an interaction between two chlorophyll molecules in the arrangement shown in Figure 7.²⁷ The arrangement of chlorophyll molecules in leaves resembles that in nano spaces of FSM, which would play an important role in the enhancement of photostability.

Photoreduction of Methyl Viologen and Evolution of Hydrogen Gas.

Figure 8 shows the photoreduction of methyl

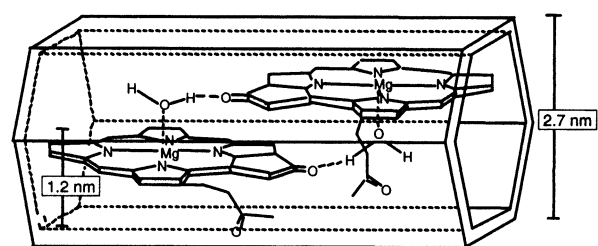


Figure 7. Tentative sketch of the arrangement of chlorophyll–FSM.

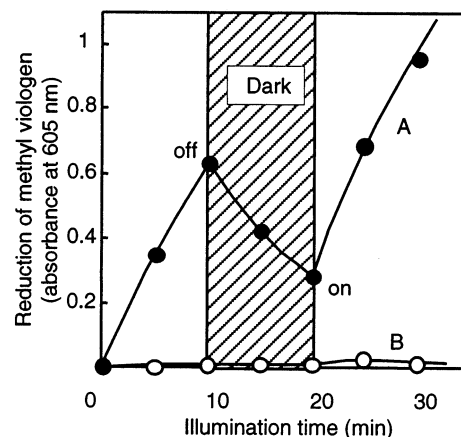


Figure 8. Photoreduction of methyl viologen by Chl–FSM (light intensity 1500 J m⁻² s⁻¹) at 30 °C. Curve A: Reaction system (3 mL) consisting of Chl–FSM (0.38 mg), methyl viologen (0.1 M), L-lysine (0.2 M), poly(vinylpyrrolidone) (1.6 mM), and 2-mercaptoethanol (1 mmol). Curve B: FSM (10 mg) was used instead of Chl–FSM in the above reaction system. The hatching in the figure indicates the period in the dark.

viologen by chlorophyll–FSM. When a suspension of chlorophyll–FSM was illuminated in the presence of 2-mercaptoethanol and methyl viologen, the absorbance at 605 nm increased with illumination time, indicating the reduction of methyl viologen (Figure 8, curve A). When the light was turned off, the absorbance at 605 nm decreased gradually, probably due to the oxidation of reduced methyl viologen by a trace amount of oxygen existing in the reaction system. When it was illuminated a second time, the absorbance increased again. On the other hand, methyl viologen was hardly reduced with only FSM in place of the chlorophyll–FSM (curve B). In the absence of L-Lys and/or poly(vinylpyrrolidone) in the reaction system, no photoreduction of methyl viologen occurred upon illumination (data not shown). The reason methyl viologen was not reduced has not been clarified yet. It is probably due to the backward

(26) Shibata, K. *Methods Biochem. Anal.* **1959**, *7*, 77–109.

(27) Rodeney, R.; Steven, G. B. *J. Am. Chem. Soc.* **1981**, *104*, 340–343.

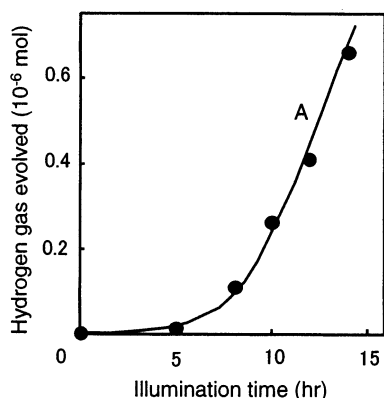
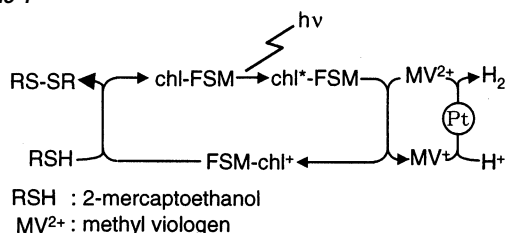


Figure 9. Hydrogen gas evolution by Chl-FSM in the presence of methyl viologen, L-lysine, poly(vinylpyrrolidone), 2-mercaptoethanol, and platinum on illumination with visible light (light intensity $380 \text{ J m}^{-2} \text{ s}^{-1}$) at 30°C . The reaction system (80 mL of 50 mM Tris-HCl buffer, pH 7.4) included Chl-FSM (200 mg), methyl viologen (50 mM), L-lysine (0.1 M), poly(vinylpyrrolidone) (1.6 mM), sodium carbonate (0.1 M), 2-mercaptoethanol (1 mmol), and platinum (0.6 mg).

Scheme 1



electron-transfer reaction from reduced methyl viologen to the chlorophyll cation radical, which was suppressed by the addition of L-Lys and poly(vinylpyrrolidone).^{28,29} As shown by curve A, approximately $86 \mu\text{mol}$ of reduced methyl viologen (MV^+) was generated in 20 min, and the reaction was still in progress. This indicates that the amount of reduced methyl viologen (MV^+) was 860 times greater than the amount of chlorophyll *a* ($0.1 \mu\text{mol}$) in the reaction system. The standard oxidation–reduction potential of methyl viologen is -0.44 V ; the photoreduction system containing the chlorophyll–FSM was expected to reduce two hydrogen ions into a hydrogen molecule according to Scheme 1.^{9,10} Figure 9 shows the hydrogen gas evolution by chlorophyll–FSM in the presence of methyl viologen (electron carrier), 2-mercaptoethanol (electron donor), and platinum on illumination with visible light. The amount of hydrogen gas evolved from the reaction system increased with the illumination time, with a delay of about 2 h, which is shown by curve A in Figure 9. After 14 h of illumination, approximately $0.65 \mu\text{mol}$ of hydrogen gas was evolved from the reaction system, and the reaction was still in progress. Therefore, the chlorophyll conjugate appears to serve as a photoactivated system that transfers electrons from 2-mercaptoethanol to the more reductive hydrogen molecule without any deterioration

during 14 h of illumination.^{9,10} A similar experiment was conducted in the absence of 2-mercaptoethanol or in the dark, but hydrogen gas was not evolved in either case (data not shown). The reason the hydrogen evolution was not observed during the initial 2 h has not been clarified yet; it is probably due to the oxidation of reduced methyl viologen by a trace amount of oxygen existing in the reaction system. Judging from these results described above, the chlorophyll conjugate excited by illumination (Chl^* conjugate) releases an electron and changes in to a cationic chlorophyll conjugate (Chl^+ conjugate). The electron reduces the methyl viologen dication (MV^{2+}) to the methyl viologen cation radical (MV^+), which reduces the hydrogen ion to hydrogen gas through the catalytic action of platinum. On the other hand, the Chl^+ conjugate is reduced by 2-mercaptoethanol to reproduce the chlorophyll conjugate (Scheme 1).

Conclusion

The success of the present study is based on finding a photostable chlorophyll *a* conjugated with FSM: chlorophyll–FSM. Generally, chlorophyll derivatives are not photostable under aerobic conditions.^{14,30} However, the chlorophyll–FSM conjugate is extensively stable in aqueous solution in comparison with chlorophyll. Furthermore, chlorophyll *a* becomes adsorbed to pores of the FSM, forming a chlorophyll–FSM conjugate, which exhibits an absorption maximum at 675 nm. Chlorophylls in intact leaves exhibit an absorption maximum of 678 nm and are quite stable against illumination. These phenomena are noteworthy, although the reasons are unclear. It is conceivable that the phenomenon is due to not only the interaction of a tetrapyrrole ring carrying magnesium with the surfaces of the pores of FSM but also the interaction between two chlorophyll molecules yielding a chlorophyll dimer (Figure 7). As mentioned above, chlorophyll molecules gained high stability against light illumination on conjugation with FSM, and the chlorophyll conjugate exhibited high photosensitizing activity during long periods of illumination. Further experiments are now in progress to stabilize the chlorophyll conjugate against light and to enhance the efficiency of the photoenergy conversion. We believe that, soon, chlorophyll molecules conjugated with multilayered compounds will be obtained to allow artificial photosynthetic reactions such as water splitting and carbon dioxide fixation.

Acknowledgment. We are grateful to Dr. Ichiro Okura, Professor, and Dr. Toshiaki Kamachi, Department of Bioengineering, Tokyo Institute of Technology, for their advice regarding the preparation of the Pt colloid. We are also deeply indebted to Dr. Shinji Inagaki, Toyota Central R & D Labs Inc., for the basic and technical advice on measurement via the photoreaction system.

JA0203059

(28) Amao, Y.; Okura, I. *J. Mol. Catal. A: Chem.* **1996**, *105*, 125–130.
 (29) Miyata, H.; Sugahara, Y.; Kuroda, K.; Kato, C. *J. Chem. Soc., Faraday Trans.* **1987**, *83*, 1851–1858.

(30) Itoh, T.; Asada, H.; Tobioka, K.; Kodera, Y.; Matsushima, A.; Hiroto, M.; Nishimura, H.; Kamachi, T.; Okura, I.; Inada, Y. *Bioconjugate Chem.* **2000**, *11*, 8–13.